AD-A058 322 PRINCETON UNIV NJ DEPT OF MECHANICAL AND AEROSPACE --ETC F/G 12/1
ERRORS IN FINITE DIFFERENCE SOLUTIONS OF NAVIER-STOKES EQUATION--ETC(U)
1978 S CHENG N00014-75-C-0376

UNCLASSIFIED NL

1 OF 1
AD A058322

END
DATE FILMED
10-78
DDC

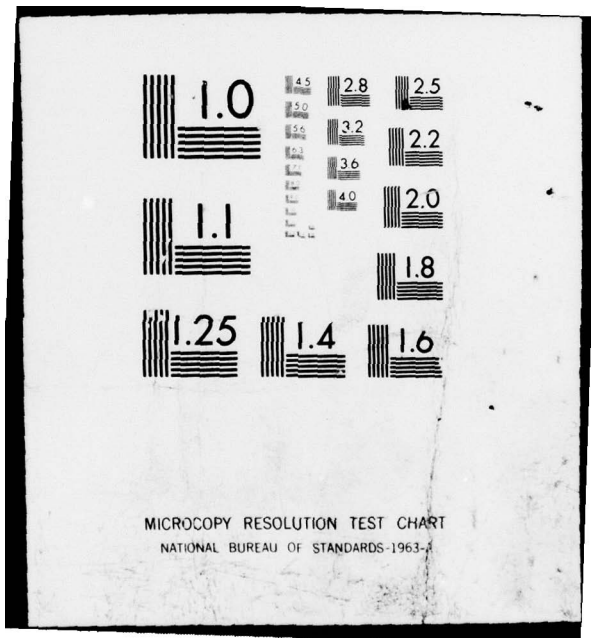
1.0
1.1
1.25
1.4
1.6
1.8
2.0
2.2
2.5
2.8
3.2
3.6
4.0
4.5
5.0
5.6
6.3
MICROCOPY RESOLUTION TEST CHART
NATIONAL BUREAU OF STANDARDS-1963-A

ERRORS IN FINITE DIFFERENCE SOLUTIONS OF NAVIER-STOKES EQUATIONS,

by

Sin-I Cheng
Department of Mechanical and Aerospace Engineering
Princeton University
Princeton, New Jersey U.S.A.

Contract N00014-75-C-0376

I. INTRODUCTION

This paper is concerned with the accuracy of numerical solutions with coarse meshes of nonlinear partial differential equations, such as the Navier-Stokes. By presuming smooth, convergent difference approximations, ~~the author carried out~~ some first differential analyses of the computational errors and ~~recommended~~ an upper error bound of $0.03\ Re\Delta x^2$ for second order accurate conservative difference schemes, computed at $Re\Delta x \lesssim 2$. In most computational solutions of complex problems, the $Re\Delta x$ is appreciably larger and the solutions are oscillatory. Neither the local truncation error nor the suggested upper bound provide any meaningful measure of the errors of the computed solution. Indeed, the computed solutions at successive mesh refinements often become "worse" and suggest possible nonuniform convergence of the sequence as $\Delta x \to 0$. Therefore we solve analytically the difference formulations of some model problems to learn about the roles of various physical and computational parameters, including the mesh Reynolds number $Re\Delta x$. The analytic results are verified by computational solutions of the model equations with various time dependent algorithms.

II. MODEL ANALYSIS

The following model problems with known exact steady state differential solutions are chosen for study.

1. Model 1: The Burgers' equation

$$u_t + uu_x = \frac{1}{Re} u_{xx} \tag{1}$$

with specified boundary values

$$u(x=0) = 0, \quad u(x=1) = -1 \tag{2}$$

2. Model 2: The same Burgers' equation with upstream boundary value and downstream extrapolation

$$u(x=-1) = 1 \quad \frac{\partial u}{\partial x}(x=1) = 0 \tag{3}$$

3. Model 3: The one-dimensional gas dynamic equations

$$\begin{cases} \rho_t + (\rho u)_x = 0 \\ (\rho u)_t + (\rho u^2)_x + p_x = \frac{1}{RE} u_{xx} \\ p = \Lambda \rho^r \end{cases} \tag{4}$$

with upstream boundary values and downstream extrapolation conditions

$$u(x=-1) = 1, \quad \rho(x=-1) = 1$$

$$\frac{\partial u}{\partial x}(x=1) = 0, \quad \text{and} \quad \frac{\partial \rho}{\partial x}(x=1) = 0 \; . \tag{5}$$

The steady state solution of (4) and (5) represents a jump from an upstream uniform flow to a downstram uniform flow with velocity Λ', which is the real solution of u from the Hugoniot relation

$$u + \Lambda/u^r = 1 + \Lambda \tag{6}$$

r is the polytropic index defining the thermodynamic process of transition and Λ is the initial data upstream.

Equations (1) and (4) are discretized according to the algorithm:

$$u_{xx} \sim (U_{j+1} - 2U_j + U_{j-1})/\Delta x^2 \tag{7a}$$

$$uu_x = (u^2/2)_x \sim \left[\gamma U_j (U_{j+1} - U_{j-1}) + (U_{j+1}^2 - U_{j-1}^2)\right]/(2+\gamma)2\Delta x \tag{7b}$$

which renders the resulting difference formulations strictly "conservative", i.e., summable without residue in the interior of the domain of summation.[2] Thus the Stokes theorem can be applied to the difference form to relate the boundary conditions explicitly with any interior point values. The difference form of Eq. (1) in the steady state is

$$U_{j+1}^2 + U_j(U_{j+1} - U_{j-1}) - U_{j-1}^2 = \frac{2(2+\gamma)}{Re\Delta x}\left[U_{j+1} - 2U_j + U_{j-1}\right] \tag{8}$$

The difference form of Eqs. (4) with discretization parameter γ_1 for the continuity and γ_2 for the momentum equation is

$$2\left[(\rho U)_{j+1} - (\rho U)_{j-1}\right] + \gamma\cdot\left[\rho_j(U_{j+1}-U_{j-1}) + U_j(\rho_{j+1}-\rho_{j-1})\right] = 0$$

$$2\left[(\rho U^2)_{j+1} - (\rho U^2)_{j-1}\right] + \gamma_2\left[U_j\left\{(\rho U)_{j+1} - (\rho U)_{j-1}\right\} + (\rho U)_j(U_{j+1}-U_{j-1})\right]$$

$$+ \Lambda\left[(\rho_{j+1})^r - (\rho_{j-1})^r\right] = \frac{2(2+\gamma_2)}{RE\Delta x}\left[U_{j+1}-2U_j+U_{j-1}\right] \quad (9)$$

The downstream extrapolation conditions are expressed as

$$U_J = U_{J-1} \quad \rho_J = \rho_{J-1}\ , \text{ etc.} \quad (10)$$

There are other algorithms that lead to strictly conservative difference formulations for complicated nonlinear terms.

Real solutions of each model system of equations are obtained analytically as follows:

1. Obtain exact solution(s) of the system for special values of $Re\Delta x$ (or $RE\Delta x$) such as $\hat{Re}\Delta x$, $\tilde{Re}\Delta x$, ... $\hat{Re}\Delta x$
2. Identify the region of rapid variation (or jump) in the exact solution in which the fully nonlinear difference relations must be taken.
3. Obtain linearized small perturbation solutions of the difference equations system about the exact solution in its region of small variation, generally including the boundary. The linearized solution serves to relate the boundary values to those function values where the linear region joins the nonlinear (or jump) region in the interior.
4. Sum up all the difference relations over the entire domain to relate the boundary values.
5. Obtain all the real sets of solutions of the function values from as many algebraic equations deduced in 2 through 4.
6. Asymptotic results for finite but large $Re\Delta x$ are studied with or without explicit solution(s) of the nonlinear system of algebraic equations.

For practical range of $Re\Delta x > 10$, the one term asymptotic results give simple functional dependence of the error of the "exact difference solution" compared with the "exact differential solution". Such an analysis is illustrated in Ref. 3 for Model 1 and detailed in Ref. 4 for the other cases. The analytical results have been verified by digital computations with the time dependent schemes of Brailovskaya,[5] of Victoria-Widhopf,[6] of Peyret-Viviand,[7] and of Cheng-Allen,[1] all with the same conservative steady state equation (8). All the computed results under the same steady state criterion agree with one another and with the analytic

estimates to three significant figures. As shown in Fig. 1, the errors of computed results for negative values of γ increases to some maximum at $Re\Delta x \sim 3$ and then reaches some minimum at larger $Re\Delta x$. The solutions in different ranges of $Re\Delta x$ are illustrated in Fig. 2. Similar results for Model 2 and Model 3 are given in Figs 3 and 4 and in Figs. 5 to 7, respectively. When the time dependent scheme like MacCormack is used, which does not reduce to (8) in the steady state, the error increases monotonically as $\sim 0.06\ Re\Delta x^2$ without plateau or extrema as $Re\Delta x$ increases (Fig. 1). The presence of error minimum at suitable large $Re\Delta x$ values may be a characteristic of the strictly conservative difference formulation.

III. ANALYTIC INFERENCES

The following qualitative inferences pertinent to practical computations may be obtained from the results of the above model study:

1. It is generally sufficient to compute with 8 - 10 mesh points within the characteristic length of the problem when $Re\Delta x$ is in the appropriate range. Many more mesh points do not improve the accuracy of the computed results at the same $Re\Delta x$.

2. There exist for a certain class of difference formulation critical mesh Reynolds numbers ($\hat{Re}\Delta x$, $\overset{*}{Re}\Delta x$, etc.) at which computations will yield smooth but abrupt jump solutions with one or more mesh points within the jump. They can be excellent approximate solutions at coarse mesh, although solutions with minimal error occur at slightly different values of $Re\Delta x$. For suitable choices of the algorithm, the trough of the error curve around $\overset{*}{Re}\Delta x$ can be flat so that computations in a broad range of values of $Re\Delta x$ can yield results as accurate as what might be expected from smooth solutions at $Re\Delta x \sim 1$.

3. The magnitudes of these critical $Re\Delta x$ can be determined a priori for the model problems. They depend on the γ's representing the higher order details of the difference algorithms. The value of $\overset{*}{Re}\Delta x$ depends more importantly on the discretization parameter (γ_1) for the continuity equation than on γ_2 of the momentum equation (Fig. 6). The thermodynamic variables in the polytropic relation in (4) appears unimportant.

4. With proper boundary formulation (such as Model 1), computations at $Re\Delta x \lesssim 1$ (or $< \tilde{Re}\Delta x$) yield smooth and accurate results with an upper bound of $\sim 0.03\ Re\Delta x^2$ as is determined from the first differential analysis.[1] The sequence appears to converge to the correct solution as $Re\Delta x \to 0$. Computational results at $Re\Delta x > \tilde{Re}\Delta x$ are oscillatory and may or may not exhibit minimum error at some critical $Re\Delta x > \tilde{Re}\Delta x$.

5. With uncertain boundary formulation (such as downstream extrapolation in Models 2 and 3), smooth computed solutions will be obtained at $Re\Delta x < \widetilde{Re}\Delta x$ but they give wrong Hugoniot or jump magnitudes. The sequence of solutions can "converge" to the wrong solution as $Re\Delta x \to 0$. The oscillatory computed solutions at $Re\Delta x > \widetilde{Re}\Delta x$ appears to diverge as $Re\Delta x$ decreases toward $\widetilde{Re}\Delta x$. But, at or near the suitable critical $Re\Delta x$ under proper choices of γ's, they can provide excellent "asumptotic approximations" with small maximal errors; quite acceptable in practice.

The above inferences are drawn from the study of only the one-dimensional model equations, and discretized only in strictly conservative difference formulations. They are not expected to apply if the difference formulation is non-conservative since Stokes' theorem is crucial to the analysis. They are, however, hoped to hold without serious modifications for more complex equation systems in multi-space dimensions. For the latter purpose, we shall only present some numerical evidences.

IV. TWO DIMENSIONAL COMPUTATIONS WITH NAVIER-STOKES EQUATIONS

The propagation of an oblique, planar shock wave in a uniform supersonic stream at M = 2 and its eventual reflection from an inviscid wall have been computed at various mesh Reynolds numbers.[9] The simplest algorithm with $\gamma_1 = \gamma_2 = 0$ (Cheng-Allen) was adopted for discretizing the Navier-Stokes equations with downstream extrapolation conditions. Fig. 8 shows the computed results of a shock with pressure ratio $p_2/p_1 = 1.910$. If the 1-D model results should be assumed to apply to the components normal to the shock, the estimate of the critical Reynolds number $(Re\Delta n_1)crit$ based on the upstream velocity U_{1n} will be $4/\left(1 - \frac{U_{2n}}{U_{1n}}\right)$, according to the procedure in Ref. 2, p. 181. The critical Reynolds number $(Re\Delta x1)crit.$ based on the mesh size Δx in the x-direction will be 15.2 for the above case. We then observe in Fig. 8 that smooth solutions are obtained with $(Re\Delta x)/(Re\Delta x1)crit < 1$. Transition from smooth to oscillatory solutions takes place gradually when $(Re\Delta x1)/(Re\Delta x1)crit \sim 1$. The reflection of the above shock from an inviscid wall is shown in Fig. 9. The reflected shock has a pressure ratio $p_3/p_2 = 1.885$ with $(\widetilde{Re}\Delta x1) = 22.1$. The same inference concerning the transition of the smooth to oscillatory solutions is observed. Fig. 10 shows the computed pressure profiles for a weak shock with $p_2/p_1 = 1.096$ and $(\widetilde{Re}\Delta x1) = 122$. Fig. 11 gives the variation of the error norms with $Re\Delta x1$. The occurrence of an error minimum of $\lesssim 3\%$ appears when $(Re\Delta x1)/(Re\Delta x1)crit$ is between 3.1 and 6.2. This ratio compares with 2 as is shown in Fig. 7 for the case $\gamma_1=\gamma_2=0$ for the one dimensional gas dynamics model. In view of the fact that the case $\gamma_1=\gamma_2=0$ departs substantially from the optimal curve shown in Fig. 6 and that the model is in one rather than two space dimensions, the agreement is encouraging. How well the analytic inference outlined in the previous section may hold and to what extent these inferences may have to be modified when more complex problems are

solved computationally with the Navier-Stokes equations, clearly needs further study.

ACKNOWLEDGMENTS

The above investigation has been sponsored by the Office of Naval Research, U. S. Navy under Contract No. N00014-75-C-0376. The author is grateful of the continued interest and support of this research. The use of the IBM 360-91 computer, which is partially supported by the National Science Foundation and Princeton University is also gratefully acknowledged.

REFERENCES

[1]Cheng, Sin-I, "Accuracy of Difference Formulation of Navier-Stokes Equations", The Physics of Fluids, Supplement II, December 1969.

[2]Cheng, Sin-I, "A Critical Review of Numerical Solution of Navier-Stokes Equations", Lecture Notes in Physics, No. 41. Progress in Numerical Fluid Dynamics, edited by J. Wirz, Springer Verlag, 1975.

[3]Cheng, Sin-I and Shubin, Gregory, "Computational Accuracy and Mesh Reynolds Numbers", to appear in J. Comp. Physics.

[4]Shubin, Gregory, "One-Dimensional Gas Dynamic Modeling and Computational Accuracy", Ph.D. Thesis, Princeton University, 1977. A shortened version is submitted to the Journal of Computational Physics.

[5]Brailovskaya, I. Y., "A Difference Scheme for Numerical Solution of the Two-Dimensional, Nonstationary Navier-Stokes Equations for a Compressible Gas", Soviet-Physics-Diklady, Vol. 10, No. 2, 1965.

[6]Victoria, K. J. and Widhopf, G. F., "Numerical Solution of the Unsteady Navier-Stokes Equations in Curvilinear Coordinates: The Hypersonic Blunt Body Merged Layer Problem". Lecture Notes in Physics, Vol. 19, Springer Verlag, 1973.

[7]Peyret, R. and Viviand, H., "Calcul de l'Econlement d'un Fluide Visquenx Compressible Autour d'un Obstacle de Forme Parabolique". Lecture Notes in Physics, Vol. 19, Springer Verlag, 1973.

[8]MacCormack, R. W., "The Effect of Viscosity in Hypervelocity Impact Cratering", AIAA Paper No. 69, 1969.

[9]Messina, Neale A., "A Computational Investigation of Shock Waves, Laminar Boundary Layers, and their Mutual Interaction", Ph.D. Thesis, Princeton University, 1977.

CAPTIONS OF FIGURES

Fig. 1. Maximum error E_∞ as a function of mesh Reynolds number $Re\Delta x = \frac{\Delta U \Delta x}{\nu}$ for Burgers' Model with downstream boundary value.

Fig. 2. Type of solutions of Burgers' model with downstream boundary value.

Fig. 3. Type of solutions of Burgers' model with downstream extrapolation.

Fig. 4. E_∞ vs $Re\Delta x$ for Burgers' model with downstream extrapolation.

Fig. 5. Type of solutions of 1-D gas dynamics model.
(a) jump next to downstream boundary k = J-2.
(b) jump at intermediate point k < J-2.

Fig. 6. Optimal discretization parameters for 1-D gas dynamic model.

Fig. 7. E_∞ vs $Re\Delta x$, for 1-D gas dynamics model r = 1.4, k = J-1.

Fig. 8. Pressure field of an oblique shock with $p_2/p_1 = 1.910$ in Mach 2 supersonic flow.

Fig. 9. Pressure field of shock reflection from inviscid wall $p_2/p_1 = 1.910$, $p_3/p_2 = 1.885$.

Fig. 10. Pressure field of an oblique weak shock with $p_2/p_1 = 1.096$.

Fig. 11. Error norms as a function of $Re\Delta x$ for shock calculations.

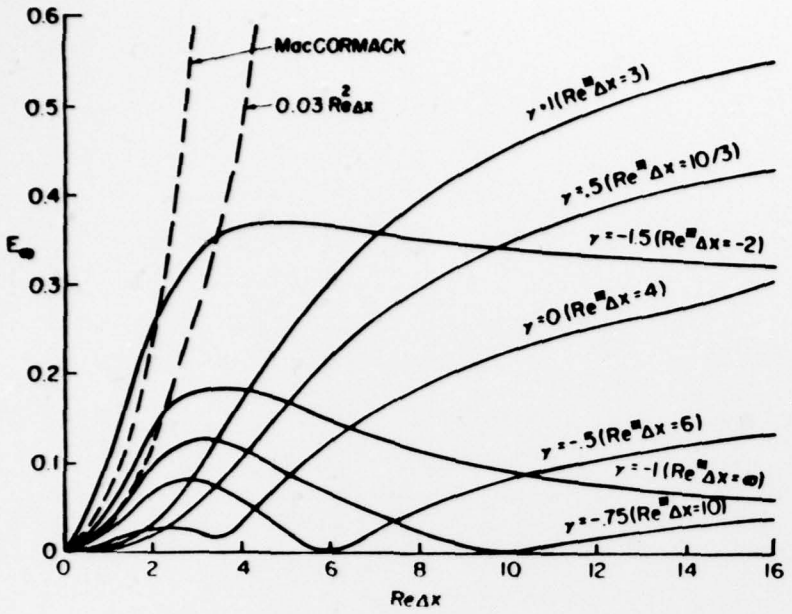

FIGURE 1

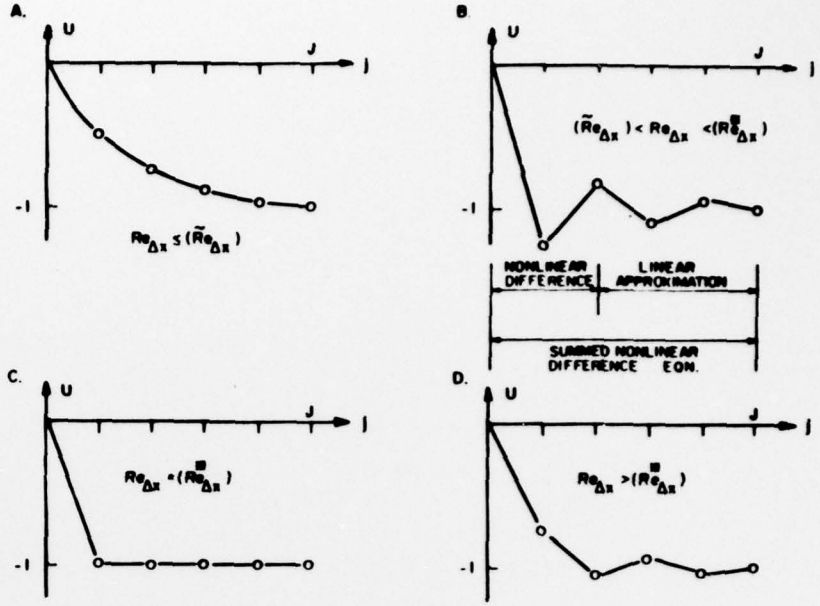

FIGURE 2

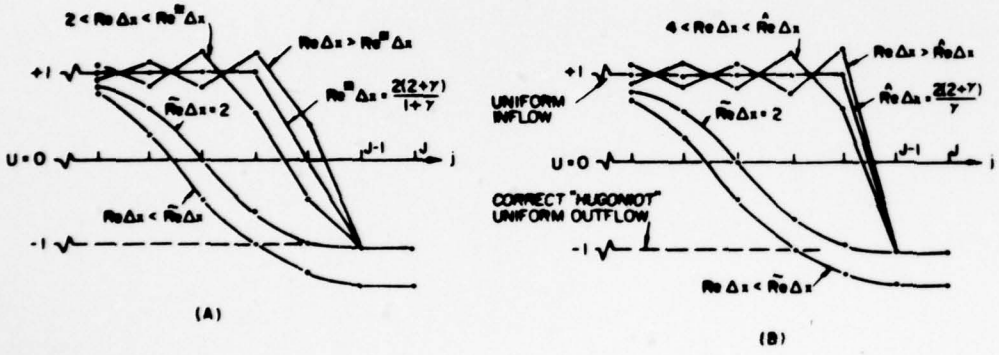

FIGURE 3

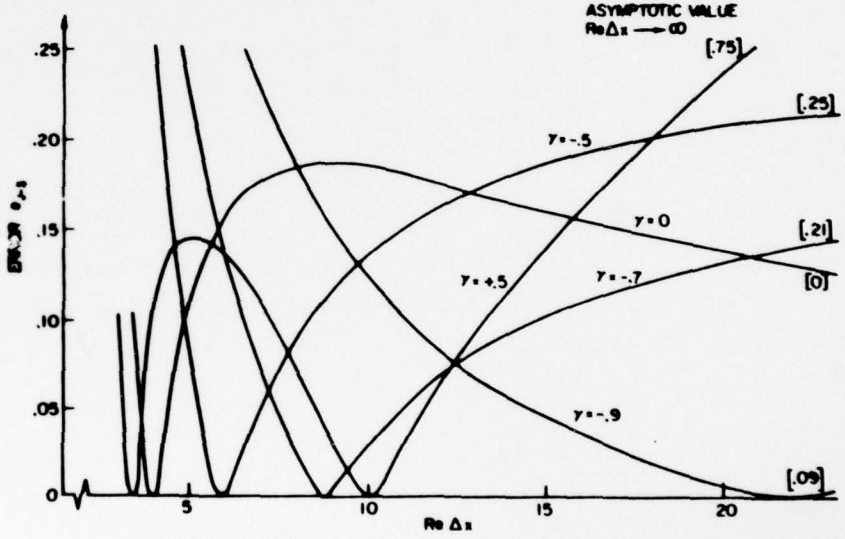

FIGURE 4

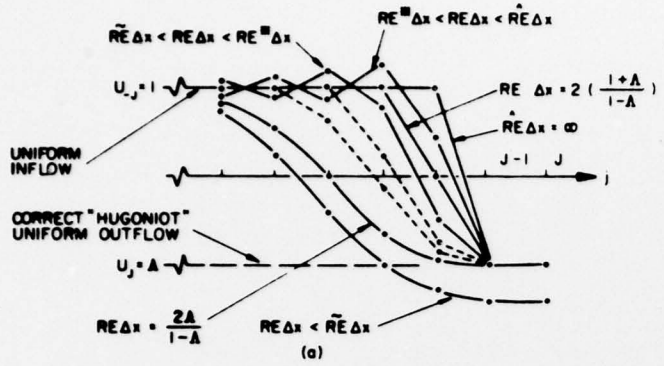

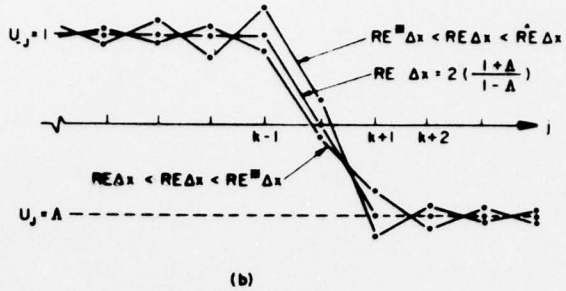

FIGURE 5

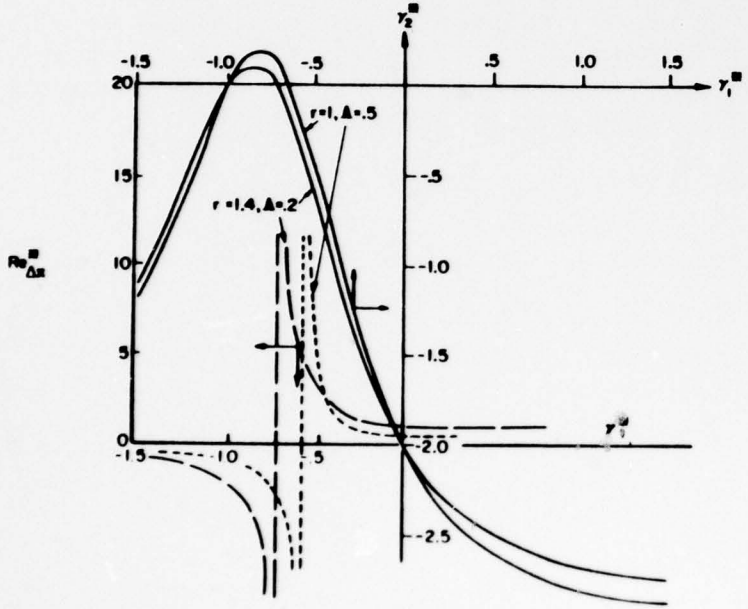

FIGURE 6

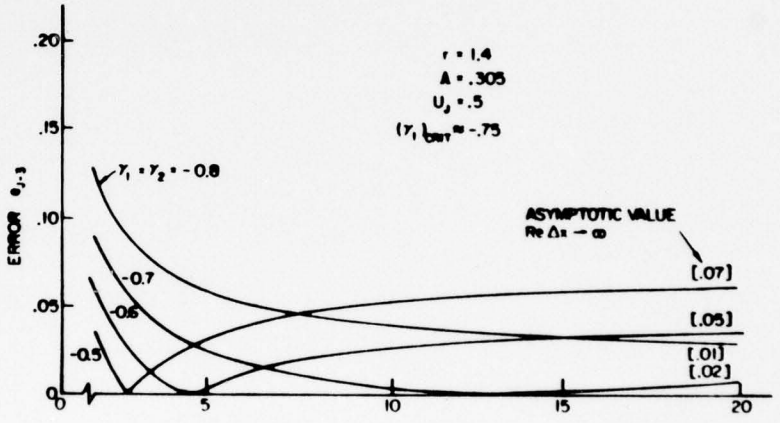

FIGURE 7

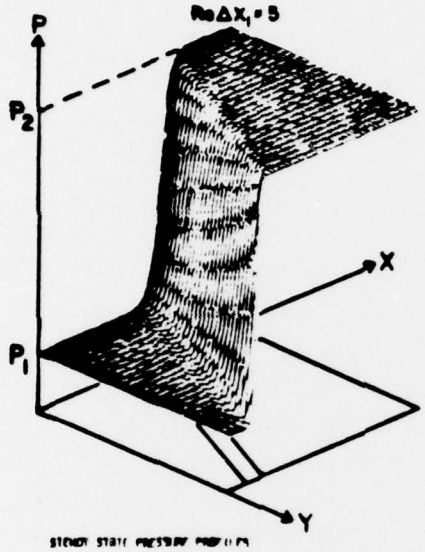

STEADY STATE PRESSURE PROFILES

A

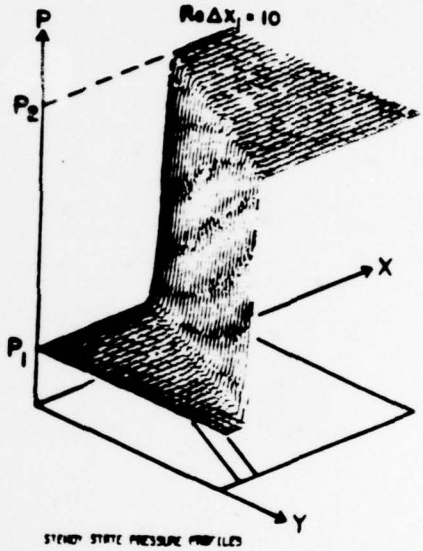

STEADY STATE PRESSURE PROFILES

B

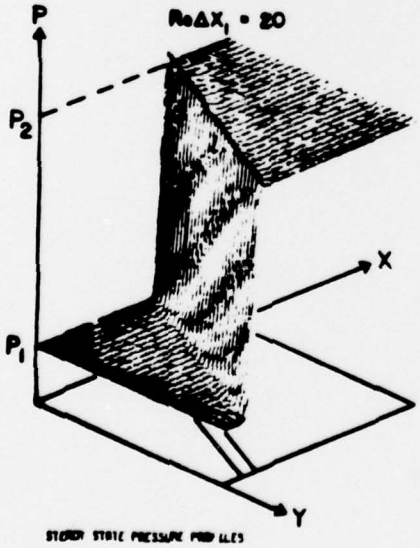

STEADY STATE PRESSURE PROFILES

C

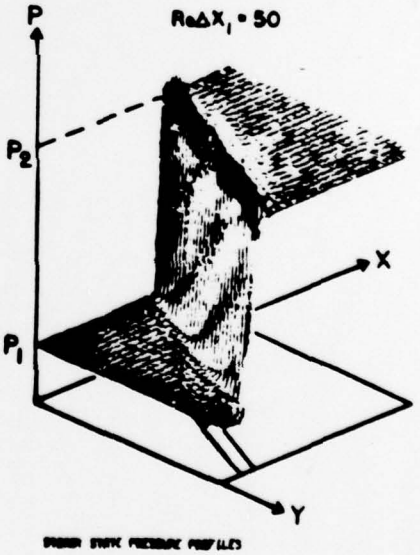

STEADY STATE PRESSURE PROFILES

D

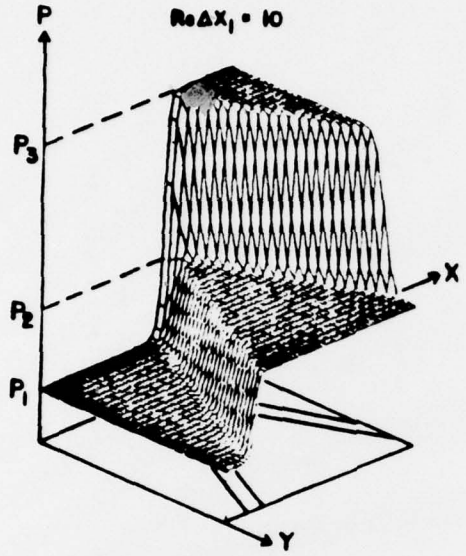

STEADY STATE PRESSURE PROFILES

A

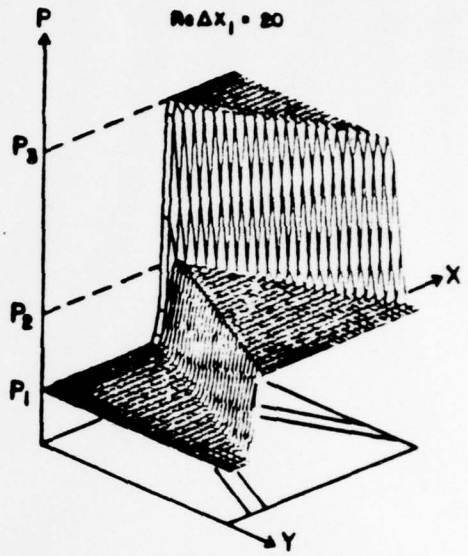

STEADY STATE PRESSURE PROFILES

B

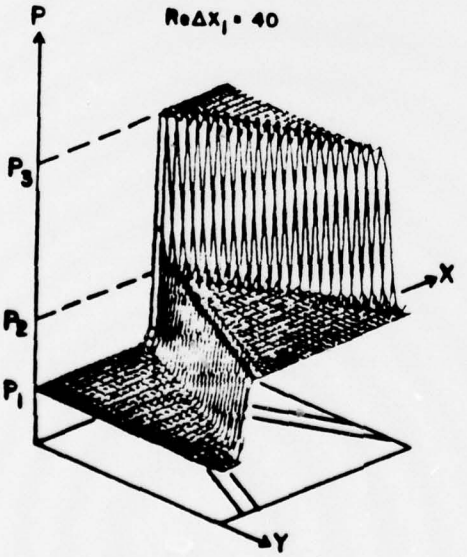

STEADY STATE PRESSURE PROFILES

C

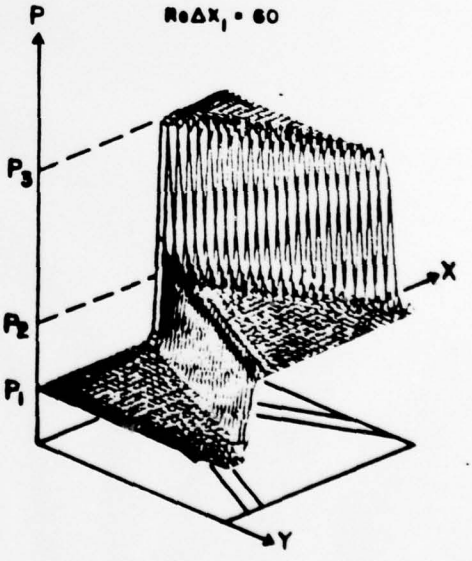

STEADY STATE PRESSURE PROFILES

D

$(Re\Delta X)_1 = 1505$

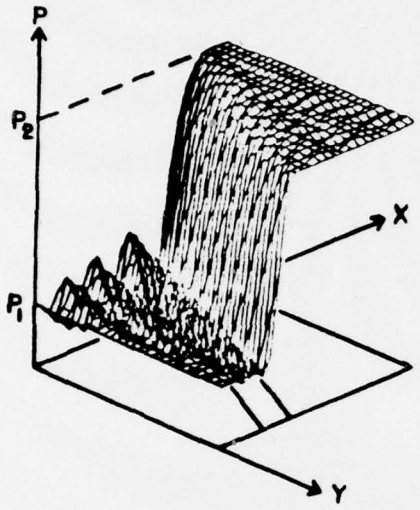

STEADY STATE PRESSURE PROFILES

A

$(Re\Delta X)_1 = 752.5$

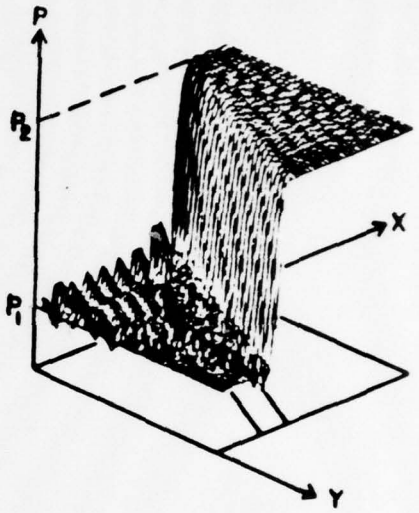

STEADY STATE PRESSURE PROFILES

B

$(Re\Delta X)_1 = 376.25$

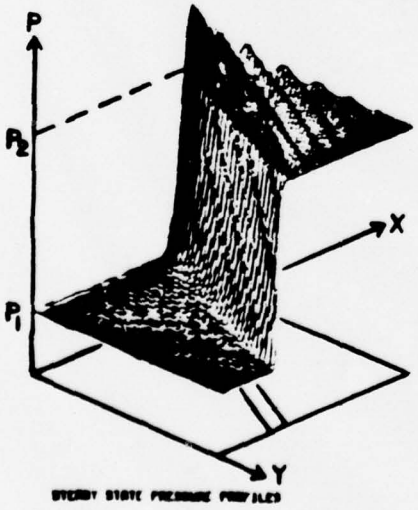

STEADY STATE PRESSURE PROFILES

C

$(Re\Delta X)_1 = 188.125$

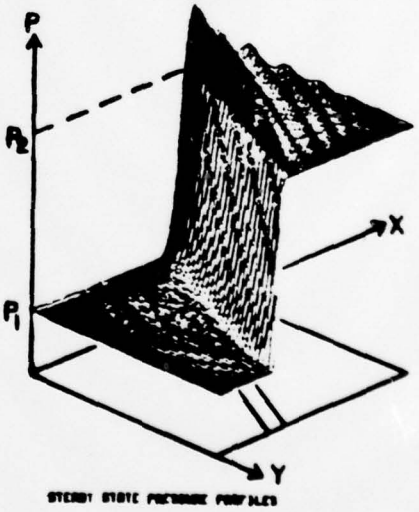

STEADY STATE PRESSURE PROFILES

D

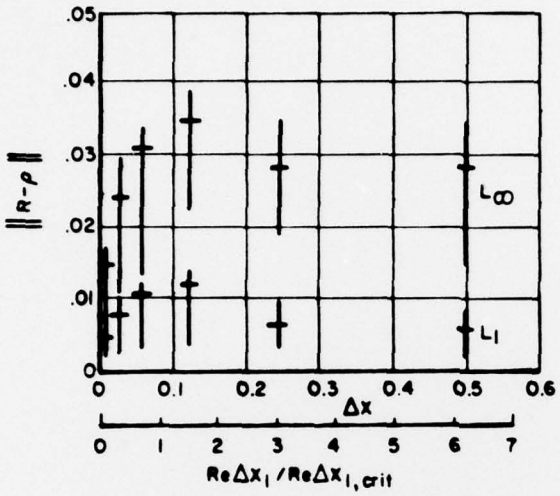
.05
.04
.03
.02
.01
0
$\|R-\rho\|$
L_∞
L_1
0 0.1 0.2 0.3 0.4 0.5 0.6
Δx
0 1 2 3 4 5 6 7
$Re\Delta x_1 / Re\Delta x_{1,crit}$

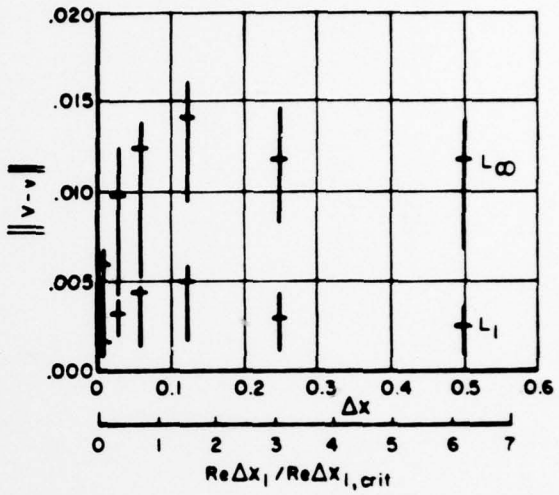
.020
.015
.010
.005
.000
$\|v-v\|$
L_∞
L_1
0 0.1 0.2 0.3 0.4 0.5 0.6
Δx
0 1 2 3 4 5 6 7
$Re\Delta x_1 / Re\Delta x_{1,crit}$

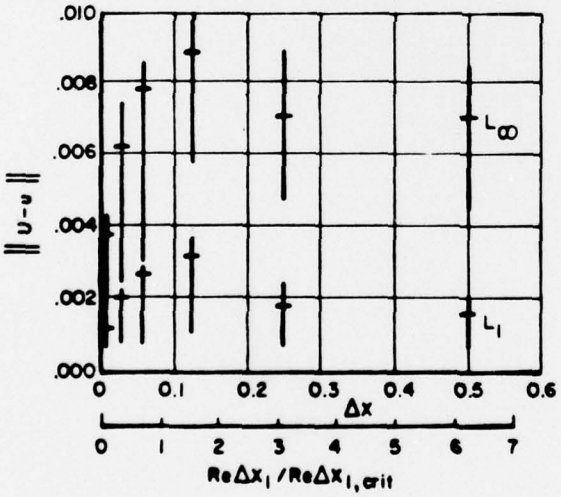
.010
.008
.006
.004
.002
.000
$\|u-u\|$
L_∞
L_1
0 0.1 0.2 0.3 0.4 0.5 0.6
Δx
0 1 2 3 4 5 6 7
$Re\Delta x_1 / Re\Delta x_{1,crit}$

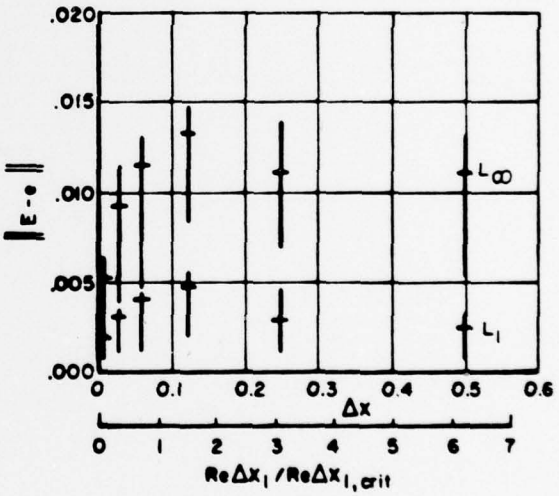
.020
.015
.010
.005
.000
$\|E-e\|$
L_∞
L_1
0 0.1 0.2 0.3 0.4 0.5 0.6
Δx
0 1 2 3 4 5 6 7
$Re\Delta x_1 / Re\Delta x_{1,crit}$